Insertion of CS$_2$ into the Group 2 metal–alkoxide bonds of [{M(OR)$_2$}$_n$] (M = Mg, Ca, Sr or Ba; R = Et or Pr^i); crystal structures of [Ca(S$_2$COPr^i)$_2$(Pr^{i}OH)$_3$]·2Pr^{i}OH and [{Ba(S$_2$COEt)$_2$}$_\infty$]

Izoldi K. Bezougli,[a] Alan Bashall,[b] Mary McPartlin[b] and D. Michael P. Mingos[a]

[a] Department of Chemistry, Imperial College of Science Technology and Medicine,
South Kensington, London, UK SW7 2AY
[b] School of Applied Chemistry, University of North London, Holloway Road, London,
UK N7 8DB

The insertion of carbon disulfide into the M–O bonds of the alkaline-earth-metal ethoxides and isopropoxides has been studied. The resulting products have been characterised by IR, ^{1}H and ^{13}C NMR spectroscopy, mass spectrometry and thermogravimetric analysis. Two of these complexes have been structurally characterised by single crystal X-ray crystallography and the data have confirmed the insertion of CS$_2$ into both Ba–O bonds of [{Ba(OEt)$_2$(EtOH)$_4$}$_n$] giving the polymer [{Ba(S$_2$COEt)$_2$}$_\infty$] and into both Ca–O bonds of [{Ca(OEt)$_2$(EtOH)$_4$}$_n$] giving the monomer [Ca(S$_2$COPr^i)$_2$(Pr^{i}OH)$_3$]·2Pr^{i}OH.

Carbon disulfide has proved to be a very versatile ligand which forms complexes with almost every transition metal.[1] A large number of carbon disulfide metal complexes have been prepared and several review articles have been devoted to their co-ordination chemistry.[1–6] Carbon disulfide has the potential to insert into a variety of M–X bonds (X = H, C, N, P, S, Cl or O),[2,7] more specifically its insertion into M–O bonds of alkoxides leads to the formation of either metal *O*-alkyl thiocarbonates or dithiocarbonates. The chemical literature has very many structurally characterised alkyl dithiocarbonato complexes of the transition metals, but very little is known about the analogous complexes of the alkaline-earth metals. In this paper we report the insertion reactions of CS$_2$ into the M–O bonds of the Group 2 metal ethoxides and isopropoxides.

Experimental

General procedures

All manipulations were carried out under an atmosphere of dry nitrogen using standard glove-box (Miller-Howe FF160) and Schlenk techniques. All solvents were rigorously dried and deoxygenated by standard procedures.

The samples for NMR, infrared studies and thermogravimetric analysis were handled in a glove-box, but those for microanalysis were not. This has led to some differences concerning the extent to which alcohol molecules of crystallization were detected by the spectroscopic and analytical techniques.

Instrumentation

Infrared spectra were recorded on a Perkin-Elmer FTIR 1720 spectrometer using Nujol mulls between 25 × 4 mm CsI plates. The Nujol was dried with 4 Å molecular sieves prior to use (and stored in a glove-box); the samples were protected from the atmosphere by an O-ring-sealed Presslok holder (Aldrich Chemicals). The NMR spectra were recorded on a JEOL GS 270 MHz spectrometer; ^{1}H NMR was referenced internally to the residual ^{1}H impurity present in the deuteriated solvent. Chemical shifts are recorded in parts per million (δ) relative to SiMe$_4$ (δ 0) using (CD$_3$)$_2$SO (δ 2.52), ^{13}C NMR to (CD$_3$)$_2$SO (δ 40.6).

Controlled thermal analyses of the complexes were investigated using a Polymer Laboratories 1500H simultaneous thermal analyser, controlled by an OmniPro 486DX-33 personal computer. The mass of the samples was between 10 and 25 mg. The measurements were carried out in alumina crucibles under an atmosphere of flowing (25 cm^3 min^{-1}) nitrogen gas, using heating rates of 5 °C min^{-1}.

Starting materials

Dibutylmagnesium, calcium, strontium and barium granules from Aldrich Chemicals Co. were used as received.

Preparations

[{Mg(S$_2$COEt)$_2$(EtOH)$_x$}$_n$] 1. Dibutylmagnesium in heptane (20 cm^3, 1 M, 20 mmol) was added to ethanol (30 cm^3) at −40 °C resulting in an exothermic reaction. The reaction mixture was slowly warmed to room temperature where the volume of the solvent was reduced until all the heptane had been removed and precipitation of a white solid [{Mg(OEt)$_2$(EtOH)$_x$}$_n$] was observed. Addition of ethanol (30 cm^3) resulted in a suspension of the magnesium ethoxide. Carbon disulfide (3.10 cm^3, 50 mmol) was added and was stirred for 12 h at room temperature. This resulted in dissolution of the ethoxide to yield a yellow solution, which was filtered to remove any insoluble species. A crystalline solid was isolated after cooling the solution to −20 °C (yield: 3.87 g, 66.7%) (Found: C, 31.3; H, 6.7. Calc. for C$_{10}$H$_{24}$MgO$_5$S$_4$: C, 31.9; H, 6.4%) [analysis based on Mg(S$_2$COEt)$_2$(EtOH)$_2$·H$_2$O]. IR (cm^{-1}) (Nujol): 3362s, 1261w, 1184s, 1120m, 1042s, 1009m, 883s, 802m, 722w, 561s and 491w. NMR [(CD$_3$)$_2$SO, 20 °C]: ^{1}H (270 MHz), δ 4.38 (t, CH$_3$CH$_2$OH, 3 H), 4.24 (q, S$_2$COCH_2CH$_3$, 4 H), 3.46 (m, CH$_3$CH_2OH, 6 H), 1.19 (t, S$_2$COCH$_2$CH_3, 6 H) and 1.07 (t, CH_3CH$_2$OH, 9 H); ^{13}C-{^{1}H} (67.94 MHz), δ 230.49 (S$_2$COR), 66.63 (S$_2$CO-CH$_2$CH$_3$), 56.68 (CH$_3$$CH_2$OH), 19.21 ($CH_3CH_2$OH) and 15.17 (S$_2$COCH$_2$$CH_3$). Mass spectrum: (positive-ion FAB), *m/z* 176, [Mg(S$_2$C)$_2$]; (negative-ion FAB), *m/z* 232, [Mg$_2$(S$_2$CO)$_2$] and 289, [Mg$_2$(S$_2$COEt)$_2$]$^-$.

[{Ca(S$_2$COEt)$_2$(EtOH)$_x$}$_n$] 2. Calcium metal (1.32 g, 32.95 mmol) was suspended in ethanol (50 cm^3) and the mixture heated under reflux for 4 h resulting in dissolution of the metal and evolution of hydrogen gas. Carbon disulfide (5.20 cm^3, 82.40

mmol) was added to the resulting suspension of [{Ca(OEt)₂-(EtOH)ₓ}ₙ] in ethanol and the solution stirred for 8 h at room temperature. This resulted in dissolution of the ethoxide to yield a yellow solution which was filtered. A crystalline solid was isolated after cooling the solution to −20 °C (yield: 4.71 g, 50.7%) (Found: C, 31.2; H, 5.8. Calc. for $C_{18}H_{38}Ca_2O_7S_8$: C, 30.8; H, 5.5%) [analysis based on $Ca_2(S_2COEt)_4(EtOH)_3$]. IR (cm⁻¹) (Nujol): 3229m, 1268w, 1177s, 1119s, 1079m, 1039s, 1011s, 875s, 803m, 771w, 723m, 674w, 655m, 446m, 372w and 320m. NMR [(CD₃)₂SO, 20 °C]: ¹H (270 MHz), δ 4.38 (s, CH_3CH_2OH, 3 H), 4.23 (q, $S_2COCH_2CH_3$, 4 H), 3.45 (q, CH_3CH_2OH, 6 H), 1.18 (t, $S_2COCH_2CH_3$, 6 H) and 1.06 (t, CH_3CH_2OH, 9 H); ¹³C-{¹H} (67.94 MHz), δ 230.48 (S_2COEt), 66.67 ($S_2COCH_2CH_3$), 56.70 (CH_3CH_2OH), 19.23 (CH_3CH_2-OH) and 15.19 ($S_2COCH_2CH_3$). Mass spectrum: (positive-ion FAB), m/z 161, [Ca(S₂COEt)]; 206, [Ca(CS)(S₂COEt)]⁺; 238, [Ca(CS₂)(S₂COEt)]⁺; 329, [Ca(S₂COEt)(EtOH)]⁺; 467, [Ca(S₂COEt)₂(EtOH)₄]⁺; 499, [CaS(S₂COEt)₂(EtOH)₄]; 551, [Ca₂(CS)(S₂COEt)₂(EtOH)₄]⁺; 583, [Ca₂(CS₂)(S₂COEt)₂(EtOH)₄]⁺ and 565, [Ca₂(S₂COEt)₄]⁺.

[{Sr(S₂COEt)₂(EtOH)ₓ}ₙ] 3. A similar experimental procedure was adopted to that described for complex **2**, starting from strontium metal (1.61 g, 18.37 mmol) in ethanol (60 cm³) and adding carbon disulfide (2.86 cm³, 46.0 mmol). In this case the reaction was exothermic, yielding a clear yellow solution within 5 min of addition of CS₂ to the strontium ethoxide solution (yield: 4.77 g, 78.8%) (Found: C, 24.4; H, 4.2. Calc. for $C_8H_{16}O_3S_4Sr$: C, 25.6; H, 4.3%) [analysis based on $Sr(S_2COEt)_2(EtOH)$]. IR (cm⁻¹) (Nujol): 3355w (br), 1290w, 1176s, 1066s, 1037s, 869m, 802m, 738w and 723w. NMR [(CD₃)₂SO, 20 °C]: ¹H (270 MHz), δ 4.41 (s, CH_3CH_2OH, 1 H), 4.26 (q, $S_2CO-CH_2CH_3$, 4 H), 3.48 (q, CH_3CH_2OH, 2 H), 1.22 (t, $S_2CO-CH_2CH_3$, 6 H) and 1.10 (t, CH_3CH_2OH, 3 H); ¹³C-{¹H} (67.94 MHz), δ 231.28 (S_2COR), 67.38 ($S_2COCH_2CH_3$), 57.45 (CH_3CH_2OH), 19.98 (CH_3CH_2OH) and 15.94 ($S_2COCH_2CH_3$). Mass spectrum: (positive-ion FAB), m/z 165, [Sr(CS₂)]⁺; 240, [Sr(CS₂)₂]; 394, [Sr(S₂COEt)₂S₂]; 615, [Sr₂(S₂COEt)₃(CS₂)] and 631, [Sr₂(S₂COEt)₃(S₂CO)]; (negative-ion FAB), m/z 375, [Sr(S₂COEt)₂(EtOH)]⁻; 407, [Sr(S₂COEt)₂S(EtOH)]⁻; 438, [Sr(S₂COEt)₂S₂(EtOH)]⁻; 451, [Sr(S₂COEt)₂(CS₂)(EtOH)]⁻; 467, [Sr(S₂COEt)₂(S₂CO)(EtOH)]⁻ and 483, [Sr(S₂COR)₂(S₂CO)O(EtOH)].

[{Ba(S₂COEt)₂}∞] 4. A similar synthetic method to that described for complex **2** was used here, starting from barium metal (1.47 g, 10.70 mmol) in ethanol (60 cm³) and adding carbon disulfide (1.66 cm³, 26.76 mmol) (yield: 2.81 g, 69.2%) (Found: C, 18.9; H, 2.6. Calc. for $C_6H_{10}BaO_2S_4$: C, 20.0; H, 2.7%) [analysis based on $Ba(S_2COEt)_2$]. IR (cm⁻¹) (Nujol): 3328w, 3185w, 1297w, 1261w, 1168s, 1143m, 1099s, 1083s, 1060s, 1043s, 1016m, 879w, 804w, 723s, 588w, 487w, 449w and 318w. NMR [(CD₃)₂SO, 20 °C]: ¹H (270 MHz), δ 4.35 (t, ROH, 1.5 H), 4.21 (q, $S_2COCH_2CH_3$, 4 H), 3.42 (dq, CH_3CH_2OH, 3 H), 1.16 (t, $S_2COCH_2CH_3$, 6 H) and 1.03 (t, CH_3CH_2OH, 4.5 H); ¹³C-{¹H} (67.94 MHz), δ 230.39 (S_2COR), 66.59 ($S_2CO-CH_2CH_3$), 56.58 (CH_3CH_2OH), 19.12 (CH_3CH_2OH) and 15.07 ($S_2COCH_2CH_3$). Mass spectrum: (positive-ion FAB), m/z 259, [Ba(S₂COEt)]⁺; 518, [Ba₂(S₂COEt)₂]⁺; 638, [Ba₂(S₂COEt)₃]⁺ and 760, [Ba₂(S₂COEt)₄]⁺; (negative-ion FAB), m/z 121, (S₂COEt, 87%) and 322, [Ba(S₂COEt)S₂].

[{Mg(S₂COPrⁱ)₂(PrⁱOH)ₓ}ₙ] 5. Dibutylmagnesium in heptane (10 cm³, 1 M, 10 mmol) was added to PrⁱOH (30 cm³) at −40 °C resulting in an exothermic reaction. The reaction mixture was slowly warmed to room temperature and the volume of the solvent reduced until all the heptane was removed and precipitation of white [{Mg(OPrⁱ)₂(PrⁱOH)₄}ₙ] was observed. Addition of PrⁱOH (30 cm³) resulted in a suspension of the magnesium

isopropoxide. Carbon disulfide (1.50 cm³, 25 mmol) was added and the solution stirred at 80 °C for 12 h. This afforded a yellow precipitate which was isolated by filtration (yield: 1.81 g, 61.6%) (Found: C, 33.0; H, 6.1. Calc. for $C_8H_{14}MgO_2S_4$: C, 32.6; H, 4.8%) [analysis based on $Mg(S_2COPr^i)_2$]. IR (cm⁻¹) (Nujol): 1365s, 1348m, 1259w, 1162s, 1149s, 1042s, 987s, 831m, 794w, 580s, 520m and 433m. NMR [(CD₃)₂SO, 20 °C]: ¹H (270 MHz), 4.29 [s, $(CH_3)_2CHOH$], 3.75 [m, $S_2COCH(CH_3)_2/(CH_3)_2-CHOH$], 1.04 [d, $S_2COCH(CH_3)_2$] and 1.02 [d, $(CH_3)_2CHOH$]; ¹³C-{¹H} (67.94 MHz), δ 230.11 [$S_2COCH(CH_3)_2$], 62.83 [$S_2COCH(CH_3)_2/(CH_3)_2CHOH$] and 26.47 [$(CH_3)_2CHOH/S_2COCH(CH_3)_2$]. Mass spectrum: (positive-ion FAB), m/z 355, [Mg(S₂COPrⁱ)₂(PrⁱOH)]⁺ and 414, [Mg(S₂COPrⁱ)₂(PrⁱOH)₂]; (negative-ion FAB), m/z 100, [Mg(S₂C)]; 175, [Mg-(S₂C)₂, 91%]⁻; 192, [Mg(S₂C)₂(O)]; 296, [Mg(S₂C)₂(PrⁱOH)₂]; 414, [Mg(S₂COPrⁱ)₂(PrⁱOH)₂] and 474, [Mg(S₂COPrⁱ)₂(PrⁱOH)₃].

[Ca(S₂COPrⁱ)₂(PrⁱOH)₃]·2PrⁱOH 6. Calcium metal (0.64 g, 15.98 mmol) was suspended in PrⁱOH (50 cm³) and heated under reflux for 36 h resulting in dissolution of the metal and evolution of hydrogen gas. Carbon disulfide (2.40 cm³, 39.94 mmol) was added to the resulting suspension of [{Ca(OPrⁱ)₂-(PrⁱOH)ₓ}ₙ] in PrⁱOH. The solution was stirred for 12 h at room temperature after which time dissolution of the alkoxide had occurred producing a clear yellow solution. The solution was filtered to remove any insoluble species, its volume was reduced and the product isolated as big cubic crystals at −20 °C (yield: 3.34 g, 67.5%) (Found: C, 41.5; H, 7.7. Calc. for $C_{17}H_{38}CaO_5S_4$: C, 41.6; H, 7.8%) [analysis based on $Ca(S_2COPr^i)_2(Pr^iOH)_3$]. IR (cm⁻¹) (Nujol): 3343s, 1301m, 1263w, 1189s, 1159s, 1137s, 1091s, 1037s, 948s, 906w, 815m, 723m and 659w. NMR [(CD₃)₂SO, 20 °C]: ¹H (270 MHz), δ 5.47 [m, $S_2COCH(CH_3)_2$, 2 H], 4.35 [d, $(CH_3)_2CHOH$, 5 H], 3.77 [m, $(CH_3)_2CHOH$, 5 H], 1.17 [d, $S_2COCH(CH_3)_2$, 12 H] and 1.05 [d, $(CH_3)_2CHOH$, 30 H]; ¹³C-{¹H} (67.94 MHz), δ 229.94 [$S_2COCH(CH_3)_2$], 72.71 [$S_2COCH(CH_3)_2$], 62.73 [$(CH_3)_2CHOH$], 26.00 [$(CH_3)_2CHOH$] and 22.40 [$S_2COCH(CH_3)_2$]. Solid state ¹³C NMR: δ 231.30, 230.13 [$S_2COCH(CH_3)_2$], 77.86, 77.50 [$S_2COCH(CH_3)_2$], 67.70 [$(CH_3)_2CHOH$], 26.69, 25.84 [$(CH_3)_2CHOH$], 23.11, 22.82, 22.27 [$S_2COCH(CH_3)_2$]. Mass spectrum: (positive-ion FAB), m/z 57, [CaO]; 192, [Ca(S₂CPrⁱ)O]⁺; 252, [Ca(S₂COPrⁱ)O(PrⁱOH)]⁺; 328, [CaO(S₂COPrⁱ)₂(PrⁱOH)]⁺ and 345, [CaO₂(S₂COPrⁱ)₂(PrⁱOH)]⁺; (negative-ion FAB), m/z 135, [S₂COPrⁱ].

[{Sr(S₂COPrⁱ)₂(PrⁱOH)₂}ₙ] 7. Strontium metal (0.99 g, 11.30 mmol) was suspended in PrⁱOH (40 cm³) and the mixture stirred at room temperature for 12 h resulting in dissolution of the metal and evolution of hydrogen gas, yielding a transparent slightly purple solution. The solution was filtered and into the clear solution carbon disulfide (1.7 cm³, 28.2 mmol) added. The solution turned immediately yellow and was stirred for 1 h at room temperature. The product was isolated after reducing the volume of the solution and cooling to −20 °C (yield: 3.29 g, 81.4%) (Found: C, 35.9; H, 5.0. Calc. for $C_{14}H_{30}O_4S_4Sr$: C, 35.2; H, 6.3%) [analysis based on $Sr(S_2COPr^i)_2(Pr^iOH)_2$]. IR (cm⁻¹) (Nujol): 3360m, 1615m, 1261m, 1190s, 1183s, 1173s, 1092s, 1069s, 1037s, 902m, 807w, 722m and 662w. NMR [(CD₃)₂SO, 20 °C]: ¹H (270 MHz), δ 5.46 [m, $S_2COCH(CH_3)_2$, 2 H], 4.36 [d, $(CH_3)_2CHOH$, 3 H], 3.78 [m, $(CH_3)_2CHOH$, 3 H], 1.16 [d, $S_2COCH(CH_3)_2$, 12 H] and 1.04 [d, $(CH_3)_2CHOH$, 18 H]; ¹³C-{¹H} (67.94 MHz), δ 229.94 [$S_2COCH(CH_3)_2$], 72.73 [$S_2COCH(CH_3)_2$], 62.70 [$(CH_3)_2CHOH$], 26.01 [$(CH_3)_2CHOH$] and 22.53 [$S_2COCH(CH_3)_2$]. Mass spectrum: (positive-ion FAB), m/z 240, [Sr(S₂CPrⁱ)O]⁺; 300, [Sr(S₂COPrⁱ)O(PrⁱOH)]⁺; 447, [Sr₂(S₂COPrⁱ)₂]⁺ and 581, [Sr₂(S₂COPrⁱ)₃]⁺; (negative-ion FAB), m/z 135, [S₂COPrⁱ]; 234, [Sr(S₂COPrⁱ)Cl]⁻; 370, [Sr(S₂COPrⁱ)₂Cl]⁻; 592, [Sr₂(S₂COPrⁱ)₃Cl]⁻ and 728, [Sr₂(S₂CO-Prⁱ)₄Cl]⁻.

Table 1 The IR data (cm^{-1}) for the dithiocarbonate group and ^{13}C NMR data in (CD$_3$)$_2$SO for compounds **1**–**8**

Complex		ν(C$_a$–O)	ν(CS$_2$)	ν(C$_b$–O)	δ (^{13}C) CS$_2$	CH$_2$/CH of S$_2$COR	CH$_2$/CH of ROH	CH$_3$ of ROH	CH$_3$ of CS$_2$OR
1	[{Mg(S$_2$COEt)$_2$(EtOH)$_x$}$_n$]	1184, 1120	1042, 883	1009	230.49	66.63	56.68	19.21	15.17
2	[{Ca(S$_2$COEt)$_2$(EtOH)$_x$}$_n$]	1177, 1119	1039, 875	1011	230.48	66.67	56.70	19.23	15.19
3	[{Sr(S$_2$COEt)$_2$(EtOH)$_x$}$_n$]	1176	1037, 869	1000	231.28	67.38	57.45	19.98	15.94
4	[{Ba(S$_2$COEt)$_2$}$_∞$]	1168, 1143	1043	1016	230.39	66.59	56.58	19.12	15.07
5	[{Mg(S$_2$COPr^i)$_2$(Pr^{i}OH)$_x$}$_n$]	1162, 1149	1042	987	230.11	62.83	62.83	26.47	26.47
6	[{Ca(S$_2$COPr^i)$_2$(Pr^{i}OH)$_3$}· 2Pr^{i}OH]	1189, 1159, 1137	1037, 815	948	229.94	72.71	62.73	26.00	22.40
7	[{Sr(S$_2$COPr^i)$_2$(Pr^{i}OH)$_2$}$_n$]	1190, 1183, 1173	1037	1069	229.94	72.73	62.70	26.01	22.53
8	[{Ba(S$_2$COPr^i)$_2$(Pr^{i}OH)$_2$}$_n$]	1187, 1170, 1159	1049	1039	230.07	72.87	62.75	26.32	22.72

[{Ba(S$_2$COPr^i)$_2$(Pr^{i}OH)$_2$}$_n$] 8. Barium metal (1.34 g, 9.76 mmol) was suspended in Pr^{i}OH (60 cm^3) and the mixture stirred at room temperature for 12 h which resulted in dissolution of the metal and evolution of hydrogen gas, yielding a transparent slightly purple solution. The solution was filtered and into the clear solution carbon disulfide (1.47 cm^3, 24.39 mmol) added. A yellow precipitate started forming in the solution soon after the addition of carbon disulfide. The solution was stirred for 1 h at room temperature and the product isolated as a microcrystalline yellow precipitate by filtration (yield: 2.65 g, 66.6%) (Found: C, 30.9; H, 3.1. Calc. for C$_{14}$H$_{30}$BaO$_4$S$_4$: C, 30.8; H, 5.9%) [analysis based on Ba(S$_2$COPr^i)$_2$(Pr^{i}OH)·H$_2$O]. IR (cm^{-1}) (Nujol): 1307w, 1261w, 1187s, 1170m, 1159m, 1095s, 1049s, 1039s, 904w, 800w and 723m. NMR [(CD$_3$)$_2$SO, 20 °C]: ^{1}H (270 MHz), δ 4.46 [d, (CH$_3$)$_2$CHO*H*, 2 H], 3.86 [m, (CH$_3$)$_2$C*H*OH/S$_2$COC*H*(CH$_3$)$_2$, 4 H], 1.25 [d, S$_2$COCH(C*H$_3$*)$_2$, 12 H] and 1.12 [d, (C*H$_3$*)$_2$CHOH, 12 H]; ^{13}C-{^{1}H} (67.94 MHz), δ 230.07 [S$_2$COCH(CH$_3$)$_2$], 72.87 [S$_2$CO*C*H(CH$_3$)$_2$], 62.75 [(CH$_3$)$_2$-*C*HOH], 26.32 [(*C*H$_3$)$_2$CHOH] and 22.72 [S$_2$COCH(*C*H$_3$)$_2$]. Solid state ^{13}C NMR: δ 230.59 [S$_2$*C*OCH(CH$_3$)$_2$], 81.38 [S$_2$CO-*C*H(CH$_3$)$_2$], 76.29 [(CH$_3$)$_2$*C*HOH], 24.12 [(*C*H$_3$)$_2$CHOH], 22.75 and 21.57 [S$_2$COCH(*C*H$_3$)$_2$]. Mass spectrum: (positive-ion FAB), m/z 138, [Ba]; 155, [BaO]$^+$; 273, [Ba(S$_2$COPr^i)]$^+$; 290, [Ba(S$_2$COPr^i)O]$^+$ and 681, [Ba$_2$(S$_2$COPr^i)$_3$]$^+$; (negative-ion FAB), m/z 135, [S$_2$COPr^i]; 284, [Ba(S$_2$COPr^i)C] and 420, [Ba(S$_2$COPr^i)$_2$C].

X-Ray crystallography

Data were collected using a Siemens P4 diffractometer, equipped with a Siemens LT2 low temperature device with graphite monochromated radiation using ω–2θ scans at 173 K. No significant decay in the intensity of three standard reflections measured after every 100 was observed. The data were corrected for Lorentz-polarisation factors and for absorption (ψ scans). The crystal data, data collection and refinement details are summarized in Table 4.

Both structures were solved by direct methods and in each case all non-hydrogen atoms were located from subsequent Fourier-difference syntheses. All non-hydrogen atoms were assigned anisotropic displacement parameters and refined using full-matrix least squares on F_o^2.[8] The hydrogen atoms for each of the compounds were included at calculated positions with C–H bond distances of 1.00 and 0.98 Å for the tertiary CH and methyl groups, respectively. The hydroxyl hydrogens in complex **6** were located in a Fourier-difference synthesis, and included in structure factor calculation with thermal parameters at 0.09 Å^2 but were not refined. During refinement all the hydrogens were allowed to ride on their parent atom and assigned isotropic thermal parameters equal to $1.2U_{eq}$ of the parent atom for the tertiary CH groups and $1.5U_{eq}$ for the methyl groups.

CCDC reference number 186/1052.

See http://www.rsc.org/suppdata/dt/1998/2671/ for crystallographic files in .cif format.

Results and Discussion

Synthesis

The products resulting from the reactions of the Group 2 metal ethoxides and isopropoxides [{M(OR)$_2$(ROH)$_x$}$_n$] (M = Mg, Ca, Sr or Ba; R = Et or Pr^i) with CS$_2$ are listed in Table 1 together with selected IR and ^{13}C NMR data. The metal alkoxides were synthesized by the methods established by previous research workers.[9] They are not sufficiently crystalline to have been structurally characterised, nonetheless NMR studies indicated that they are solvated and x in the general formula is either 3 or 4 depending on the nature of R.[9] Liquid carbon disulfide (2 equivalents) was added to a suspension of the metal alkoxide in alcohol and the solution stirred until dissolution of the metal alkoxide was complete and a clear yellow solution had formed [equation (1)]. The reactions were done under an

$$[\{M(OR)_2(ROH)_x\}_n] + 2CS_2 \longrightarrow$$
$$[\{M(S_2COR)_2(ROH)_x\}_n] \quad (1)$$
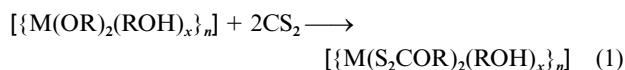
inert atmosphere and oxygen and moisture were excluded during and after the reactions.

The rates of reaction of CS$_2$ with the Group 2 metal alkoxides showed great variations depending on the specific alcohols and metals involved. The addition of CS$_2$ to ethanol solutions of Mg(OEt)$_2$ or Ca(OEt)$_2$ resulted in the dissolution of the ethoxide after stirring for 12 or 8 h, respectively. In contrast, on addition of CS$_2$ to ethanol solutions of Sr(OEt)$_2$ or Ba(OEt)$_2$ a very rapid exothermic reaction occurred, accompanied by dissolution of the alkoxides. In all cases clear yellow solutions were obtained which were filtered in order to remove any insoluble residues and compounds **1**–**4** were isolated as crystalline materials after cooling the solution to −20 °C.

In the case of Mg(OPr^i)$_2$ the alkoxide was suspended in Pr^{i}OH and after addition of CS$_2$ the reaction mixture was refluxed for 12 h. A yellow product was formed at the end of the reaction. During the preparation of the CS$_2$ calcium isopropoxide adduct the solution was stirred for 12 h after which time almost all the alkoxide had dissolved. The solution was filtered and complex **6** was isolated as a crystalline yellowish material at −20 °C. In the case of Sr(OPr^i)$_2$ and Ba(OPr^i)$_2$ the alkoxides were dissolved in Pr^{i}OH at room temperature and CS$_2$ was added to the clear colourless solutions. These solutions turned yellow and after stirring for 1 h at room temperature **7** and **8** were isolated as yellow microcrystalline solids after cooling to −20 °C.

Spectroscopic characterisation

The IR spectra of complexes **1**–**8** were studied as Nujol mulls between CsI plates and the stretching vibrations of the *O*-alkyl dithiocarbonate groups are summarised in Table 1. The infrared data have been assigned on the basis of previously reported

IR spectra of such complexes.[10] The C–O–C linkage frequencies of the ligand were separated into two ranges according to the two different carbon environments: $[S_2–C_a–O–C_b–R]^-$.

The most important features of the ^1H NMR spectra for complexes **1–8** are recorded in the Experimental section. The protons of the two different CH_2 environments of the ethyl dithiocarbonato and the ethanol ligands in **1–4** appeared as two distinct peaks at δ *ca.* 4.25 and at *ca.* 3.46, respectively. Similarly, the protons of the two different CH_3 groups appeared as two distinct triplets at δ *ca.* 1.19 for the CH_3 of the dithiocarbonato moiety, and at δ *ca.* 1.08 for the co-ordinated ethanol molecules. The OH proton was observed at higher chemical shifts, at δ *ca.* 4.38, as a triplet for **1** and **4**, and as a singlet for **2** and **3**.

Similar assignments were made for the isopropyl dithiocarbonato complexes **5–8**. The different CH environments of the isopropyl dithiocarbonato and co-ordinated Pr^{i}OH molecules appeared at δ *ca.* 5.47 and *ca.* 3.78, respectively, for **6** and **7** while the two sets of CH_3 groups were observed at δ *ca.* 1.17 and *ca.* 1.05 as distinct triplets. In contrast, in the ^1H NMR spectra of **5** and **8** the peaks associated with the two different CH environments of the isopropyl dithiocarbonato and the bound Pr^{i}OH molecules appeared in the same region as a broad multiplet at δ 3.75 and 3.86, respectively. This is believed to be due to an exchange process occurring between the Pr^{i}OH and isopropyl dithiocarbonato ligands on the NMR timescale.

The ^{13}C NMR data for complexes **1–8** in $(CD_3)_2SO$ are summarised in Table 1. They support the presence of $[S_2C(OR)]^-$ and ROH ligands. The carbon atom of the CS_2 group was observed at low field, δ *ca.* 230, for all the dithiocarbonato complexes. Free CS_2 has a ^{13}C resonance at δ 192.

Since the alkyl dithiocarbonato complexes **1–8** had low solubilities in common organic solvents it was necessary to use dimethyl sulfoxide as the solvent for the measurement of the NMR spectra. Since it is a co-ordinating solvent the NMR assignments which were obtained must be treated with some caution, nonetheless the ^1H and ^{13}C NMR data are useful for discriminating the different OR environments and therefore provide a basis for confirming the stoichiometries of the compounds. The degree of aggregation of the complexes, however, cannot be established by NMR.

Mass spectrometry

Mass spectroscopic studies by positive and negative ion fast atom bombardment (FAB$^+$ and FAB$^-$, respectively) for complexes **1–8** yielded complicated fragmentation patterns. Molecular ions were not observed, something that is believed to be due to the poor volatilities and thermal stabilities of these complexes. Nevertheless, certain complexes exhibited fragments in both FAB$^+$ and FAB$^-$ spectra consistent with the presence of $M(S_2COR)$, $M(S_2COR)_2$, $M_2(S_2COR)_2$, $M_2(SCOR)_3$ and solvated fragments of the type $M_n(S_2COR)_n(ROH)_n$ (see Experimental section). Surprisingly, in the FAB-spectra of the isopropyl dithiocarbonato complexes **6–8** the $S_2C(OPr^i)^-$ ion *m/z* 135 was observed as the most intense peak.

Thermogravimetric analysis (TGA) and differential scanning calorimetry (DSC)

Thermogravimetric analyses and differential scanning calorimetric studies were performed for all alkyl thiocarbonato complexes **1–8**.

The DSC plot of complex **1** showed one exotherm with a shoulder between 25 and 140 °C. This was associated in the TGA plot with a single rapid weight loss of 70%, corresponding to the loss of three molecules of ethanol, one molecule of $[S_2C(OR)]^-$ and a CH_2CH_3 group. The resulting intermediate was stable up to 200 °C whereupon the OCS group was elim-
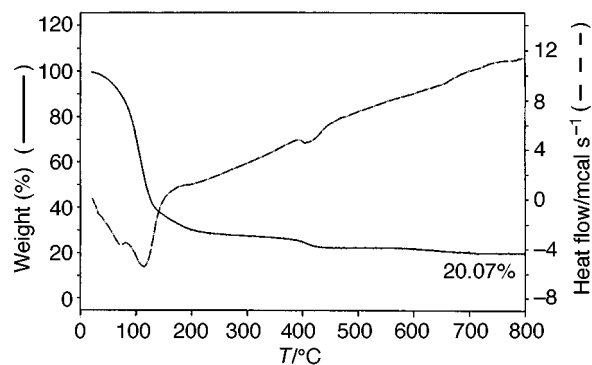

Fig. 1 The TGA/DSC curves of complex $[Ca(S_2COPr^i)_2(Pr^iOH)_3]\cdot$ $2Pr^iOH$ **6**; cal = 4.184 J

ated to yield MgS at 440 °C. The residue of 13.74% (calc. for MgS 13.86%) was stable to 800 °C. The decomposition of **5** showed a more complicated pattern. The residue (31.53%) remained as a very high percentage even at 800 °C, and possibly corresponds to $MgCS_2$ or MgS_2. The DSC plot of **2** shows one endotherm between 25 and 200 °C which is reflected in the TGA trace with a single weight loss of 70%. This corresponds to the loss of one and a half molecules of ethanol and two CSOR groups. The subsequent weight loss of 10% corresponds to the loss of one S atom to yield CaS at 400 °C (residue *ca.* 20%, calc. for CaS 20.5%). A similar decomposition pattern was obtained for **3** leaving a residue of SrS at 500 °C (observed residue 38.03%, calc. for SrS 36.29%). The DSC curve of complex **4** showed several interesting features. A broad endotherm was observed over the range 25–210 °C within which three distinct peaks were apparent; the first is centred at 55 °C, the second at 100 °C and the third at 180 °C. This was mirrored in the TGA plot with a weight loss of 38.5% corresponding to a third of an ethanol molecule, a COEt group and a CS_2 fragment to yield $[BaS_2(OEt)]$. The subsequent weight loss of 18% corresponds to the loss of the SOEt fragment to yield BaS at 500 °C (residue 42.8%, calc. for BaS 42.9%). The DSC of **6** showed two endotherms, the first centred at 70 °C and the second at 120 °C (Fig. 1). This was mirrored in the TGA plot with a single rapid weight loss of 70% corresponding to the loss of one molecule of Pr^{i}OH and two CSOR groups. The subsequent weight loss of 10% represents the decomposition of CaS_2 to CaS (residue 20.07%, calc. for CaS 19.5%). A similar decomposition pattern was observed for **7**. The TGA curve showed one major weight loss between 25 and 200 °C, representing the loss of two CSOR groups. The subsequent weight loss of *ca.* 10% represented the decomposition of SrS_2 to SrS at 800 °C (residue 32.84%, calc. for SrS 33.52%). The TGA of **8** showed a continuous weight loss between 25 and 240 °C, corresponding to the loss of one OR and one CSOR group. The second weight loss represented the loss of two S atoms to yield BaS and presumably some carbonaceous deposits at 800 °C.

In general the observation that these dithiocarbonato complexes decompose to the corresponding metal sulfides at 500 °C is not too surprising. For example. a similar decomposition pattern to that described for **6** has been previously reported for the calcium methyl dithiocarbonato complex $[\{Ca(S_2COMe)_2(MeOH)_4\}_n]$.[11] Also, Greenwood and Earnshaw[12] have described the alkaline-earth-metal sulfides MS as high melting point solids.

Crystal structures

$[\{Ba(S_2COEt)_2\}_\infty]$ 4. X-Ray single crystal analysis confirmed that the insertion of CS_2 into both Ba–O bonds of $[\{Ba(OEt)_2(EtOH)_4\}_n]$ had occurred to give the polymeric structure $[Ba(S_2COEt)_2\}_\infty]$ illustrated in Fig. 2 in which each barium ion is

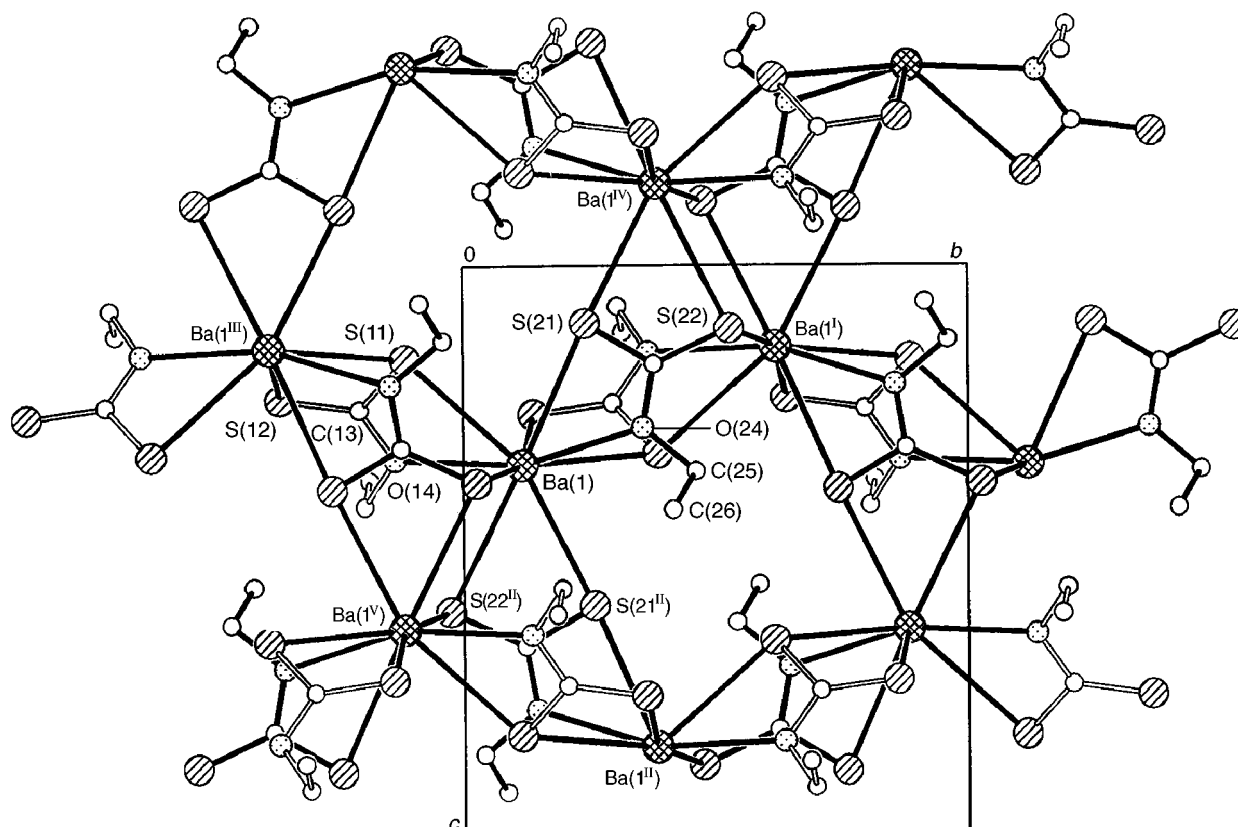**Fig. 2** Part of the polymeric structure of [{Ba(S$_2$COEt)$_2$}$_\infty$] **4** formed by CS$_2$ insertion into the Ba–O bonds of barium ethoxide showing the nine-co-ordination at barium. The Roman superscripts refer to atoms at equivalent positions listed in Table 2

nine-co-ordinate. Selected bond lengths and angles are listed in Table 2.

The asymmetric unit of the crystal consists of two ethyl dithiocarbonato ligands each linked in a bidentate mode to a barium atom *via* a sulfur atom [Ba–S(11) 3.209(1), Ba(1)–S(21) 3.237(1) Å] and the oxygen donor [Ba–O(14) 2.967(2), Ba–O(24) 3.042(2) Å]. Each ligand also bonds in chelating mode *via* both sulfur atoms to adjacent symmetry related barium ions [Ba(1^{III})–S(11) 3.237(1), Ba(1^{III})–S(12) 3.200(1); Ba(1^{IV})–S(21) 3.234(1), Ba(1^{IV})–S(22) 3.280(1) Å], and in addition one sulfur atom forms a slightly longer monodentate link to a third symmetry related barium ion [Ba(1^I)–S(22) 3.335(1) Å]. The first ligand therefore bridges two symmetry related barium atoms and the second bridges three.

[Ca(S$_2$COPr^i)$_2$(Pr^{i}OH)$_3$]·2Pr^{i}OH 6. The X-ray study of complex **6** confirmed the formation of the monomer [Ca(S$_2$CO-Pr^i)$_2$(Pr^{i}OH)$_3$]·2Pr^{i}OH resulting from the insertion of CS$_2$ into both M–O metal alkoxide bonds. The molecular structure is shown in Fig. 3 and selected bond lengths and angles are summarised in Table 3. The calcium is seven-co-ordinate with bonds to the two sulfur atoms of both S$_2$C(OPr^i)$^-$ molecules and to the oxygen atoms of three Pr^{i}OH ligands; it may be envisaged as having a distorted pentagonal bipyramidal geometry, with two Pr^{i}OH molecules in the axial sites. Two chelate ligands [mean S–Ca–S 60.85(3)°] are in the equatorial plane together with the third Pr^{i}OH ligand [deviations from mean plane Ca 0.053, S(1A) 0.069, S(1B) 0.311, S(2A) 0.141, S(2B) 0.369, O(1D) 0.321 Å]. The equatorial Ca–O distance [Ca–O(1D) 2.374 Å] is slightly longer than the distance to the two axial Pr^{i}OH [mean Ca–O 2.351(2) Å].

The two dithiocarbonato ligands are co-ordinated in a slightly asymmetric bidentate fashion each having a relatively short Ca–S bond [Ca–S(2A) 2.897(1) and Ca–S(1B) 2.886(1) Å]

Table 2 Selected bond lengths (Å) and angles (°) for complex **4**

Ba(1)–O(14)	2.967(2)	Ba(1)–O(24)	3.042(2)
Ba(1)–S(11)	3.2088(9)	S(12)–Ba(1^{III})	3.1997(10)
Ba(1)–S(21)	3.2374(9)	S(11)–Ba(1^{III})	3.2368(9)
S(21)–Ba(1^{IV})	3.2338(9)	S(22)–Ba(1^{IV})	3.2799(9)
S(22)–Ba(1^I)	3.3351(9)	S(11)–C(13)	1.707(3)
S(12)–C(13)	1.664(3)	S(21)–C(23)	1.692(3)
S(22)–C(23)	1.690(3)	O(14)–C(13)	1.350(4)
O(14)–C(15)	1.468(4)	O(24)–C(23)	1.333(4)
O(24)–C(25)	1.463(4)	C(15)–C(16)	1.506(5)
C(25)–C(26)	1.482(6)		
S(12^I)–Ba(1)–S(11)	82.03(2)	S(12^I)–Ba(1)–S(21^{II})	115.37(3)
S(11)–Ba(1)–S(21^{II})	155.97(2)	S(12^{II})–Ba(1)–S(11^I)	55.19(2)
S(11)–Ba(1)–S(11^I)	126.80(2)	S(21^{II})–Ba(1)–S(11^I)	77.08(2)
S(12^I)–Ba(1)–S(21)	86.45(3)	S(11)–Ba(1)–S(21)	72.40(2)
S(21^{II})–Ba(1)–S(21)	122.658(10)	S(11^I)–Ba(1)–S(21)	74.71(2)
S(12)–Ba(1)–S(22^{II})	109.20(2)	S(11)–Ba(1)–S(22^{II})	105.29(2)
S(21)–Ba(1)–S(22^{II})	54.64(2)	S(11)–Ba(1)–S(22^{II})	116.93(2)
S(21)–Ba(1)–S(22^{II})	163.91(3)	S(12^I)–Ba(1)–S(22^{III})	162.80(2)
S(11)–Ba(1)–S(22^{III})	80.79(2)	S(21^{II})–Ba(1)–S(22^{III})	81.34(2)
S(11^I)–Ba(1)–S(22^{III})	137.80(2)	S(21)–Ba(1)–S(22^{III})	87.55(3)
S(22^{II})–Ba(1)–S(22^{III})	76.39(2)	O(14)–Ba(1)–O(24)	162.88(6)
O(14)–Ba(1)–S(12^I)	65.59(5)	O(24)–Ba(1)–S(12^I)	111.92(5)
O(14)–Ba(1)–S(11)	48.63(5)	O(24)–Ba(1)–S(11)	114.79(5)
O(14)–Ba(1)–S(21^{II})	121.33(5)	O(24)–Ba(1)–S(21^{II})	75.50(5)
O(14)–Ba(1)–S(11^I)	119.20(5)	O(24)–Ba(1)–S(11^I)	64.78(5)
O(14)–Ba(1)–S(21)	116.00(5)	O(24)–Ba(1)–S(21)	47.39(5)
O(14)–Ba(1)–S(22^{II})	69.45(5)	O(24)–Ba(1)–S(22^{II})	125.19(5)
O(14)–Ba(1)–S(22^{II})	103.00(5)	O(24)–Ba(1)–S(22^{III})	74.94(5)

Symmetry transformations used to generate equivalent atoms:
I $x, \frac{1}{2} - y, \frac{1}{2} + z$; II $1 - x, +y, \frac{1}{2} - z$; III $x, \frac{1}{2} - y, \frac{1}{2} + z$;
IV $1 - x, -\frac{1}{2} + y, \frac{1}{2} - z$.

and a long Ca–S bond [Ca–S(1A) 2.922(1) and Ca–S(2B) 2.969(1) Å]. The longest of these bonds [Ca–S(2B)] is similar in length to the Ca–S bond [2.961(1) Å] found in the COS

Table 3 Selected bond lengths (Å) and angles (°) for complex **6**

Ca–O(1C)	2.346(2)	Ca–O(1E)	2.357(2)
Ca–O(1D)	2.374(2)	Ca–S(1B)	2.8862(9)
Ca–S(2A)	2.8974(11)	Ca–S(1A)	2.9218(11)
Ca–S(2B)	2.9694(11)	S(1A)–C(3A)	1.675(2)
S(2A)–C(3A)	1.690(3)	C(3A)–O(4A)	1.335(3)
O(4A)–C(5A)	1.462(3)	C(5A)–C(7A)	1.498(4)
C(5A)–C(6A)	1.507(4)	S(1B)–C(3B)	1.691(3)
S(2B)–C(3B)	1.671(3)	C(3B)–O(4B)	1.337(3)
O(4B)–C(5B)	1.466(3)	C(5B)–C(6B)	1.496(4)
C(5B)–C(7B)	1.507(4)	O(1C)–C(2C)	1.442(3)
C(2C)–C(3C)	1.495(4)	C(2C)–C(4C)	1.498(4)
O(1D)–C(2D)	1.431(3)	C(2D)–C(4D)	1.506(4)
C(2D)–C(3D)	1.505(4)	O(1E)–C(2E)	1.443(3)
C(2E)–C(4E)	1.495(4)	C(2E)–C(3E)	1.510(4)
O(1F)–C(2F)	1.443(3)	C(2F)–C(3F)	1.491(4)
C(2F)–C(4F)	1.499(4)	O(1G)–C(2G)	1.438(3)
C(2G)–C(3G)	1.501(4)	C(2G)–C(4G)	1.501(4)
O(1C)–Ca–O(1E)	167.77(6)	O(1C)–Ca–O(1D)	91.18(7)
O(1E)–Ca–O(1D)	76.91(6)	O(1C)–Ca–S(1B)	103.75(5)
O(1E)–Ca–S(1B)	87.30(5)	O(1D)–Ca–S(1B)	138.48(5)
O(1C)–Ca–S(2A)	86.40(5)	O(1E)–Ca–S(2A)	88.92(5)
O(1D)–Ca–S(2A)	81.02(5)	S(1B)–Ca–S(2A)	137.51(3)
O(1C)–Ca–S(1A)	95.50(6)	O(1E)–Ca–S(1A)	92.10(5)
O(1D)–Ca–S(1A)	140.80(5)	S(1B)–Ca–S(1A)	76.85(3)
S(2A)–Ca–S(1A)	61.01(3)	O(1C)–Ca–S(2B)	83.48(5)
O(1E)–Ca–S(2B)	97.74(5)	O(1D)–Ca–S(2B)	83.45(5)
S(1B)–Ca–S(2B)	60.68(3)	S(2A)–Ca–S(2B)	161.26(3)
S(1A)–Ca–S(2B)	135.65(3)	C(3A)–S(1A)–Ca	87.56(9)
C(3A)–S(2A)–Ca	88.10(9)	C(3B)–S(1B)–Ca	89.20(9)
C(3B)–S(2B)–Ca	86.78(9)	C(2C)–O(1C)–Ca	129.7(2)
Ca–O(1C)–H(1C)	122.65(12)	C(2D)–O(1D)–Ca	133.7(2)
Ca–O(1D)–H(1D)	116.44(12)	C(2E)–O(1E)–Ca	130.8(2)
Ca–O(1E)–H(1E)	122.91(13)		

Fig. 3 (a) The distorted pentagonal geometry of the CS$_2$ insertion product [Ca(S$_2$COPr^i)$_2$(Pr^{i}OH)$_3$]·2Pr^{i}OH **6**. (b) The dimer formed in the crystal of complex **6** by hydrogen bonding between an isopropyl dithiocarbonato ligand of one molecule and the proton of a co-ordinated propanol on a centrosymmetrically related molecule. The symmetry operations relating equivalent atoms are:
I −x, −y, −z; II −1 − x, −y, −z; III 1 + x, y, z

insertion product [{Ca(OCSOMe)$_2$(MeOH)$_3$}$_2$], the only other Ca–S linkage from a bidentate ligand co-ordinated to calcium that has been structurally characterised.[13]

In the solid state molecules of complex **6** form dimers, linked by hydrogen bonding between the proton of an axial Pr^{i}OH ligand of one molecule and a sulfur donor of a centrosymmetrically related molecule [H(1C)···S(2A^I) 2.223 Å] as illustrated in Fig. 3(b). The two remaining co-ordinated Pr^{i}OH ligands form a hydrogen bonded 'chelate ring' *via* hydrogen bonds from their protons to an oxygen atom of one of the solvent Pr^{i}OH [H(1D)···O(1F) 1.846 and H(1E)···O(1F) 1.906 Å]. One sulfur donor is linked *via* a relatively weak hydrogen bond to the second solvent Pr^{i}OH [S(1B)···H(1G) 2.416 Å]; hydrogen bonding also links the two solvent molecules at different equivalent positions [H(1F)···O(1G^{III}) 1.822 Å] so that the overall dimeric units are linked into polymeric chains parallel to the *a* axis.

Conclusion

This research has demonstrated the insertion of CS$_2$ into both the M–O bonds of alkaline-earth-metal alkoxides, resulting in the formation of the alkyl dithiocarbonato complexes with the general formula [{M(S$_2$COR)$_2$(ROH)$_x$}$_n$]. We have recently reported a series of Group 2 metal alkyl thiocarbonato complexes resulting from the insertion of COS into metal–alkoxide bonds.[14] The monomeric complexes [Mg(OCSOEt)$_2$(EtOH)$_4$] and [Mg(OCSOPr^i)$_2$(Pr^{i}OH)$_4$], the dimer [{Ca(OCSOMe)$_2$(MeOH)$_3$}$_2$], the 'trimer' [Sr$_3$(OCSOEt)$_6$(EtOH)$_8$] and finally the polymer [{Sr(OCSOPr^i)$_2$(Pr^{i}OH)$_2$}$_\infty$] have demonstrated how the nuclearity increases with an increase in the ionic radius of the metal ion. Moving from Mg^{2+}, to Ca^{2+} to Sr^{2+}, there is a preference for higher co-ordination numbers which are achieved by oligomerisation or polymerisation processes. A similar trend has resulted from the study of the two structurally
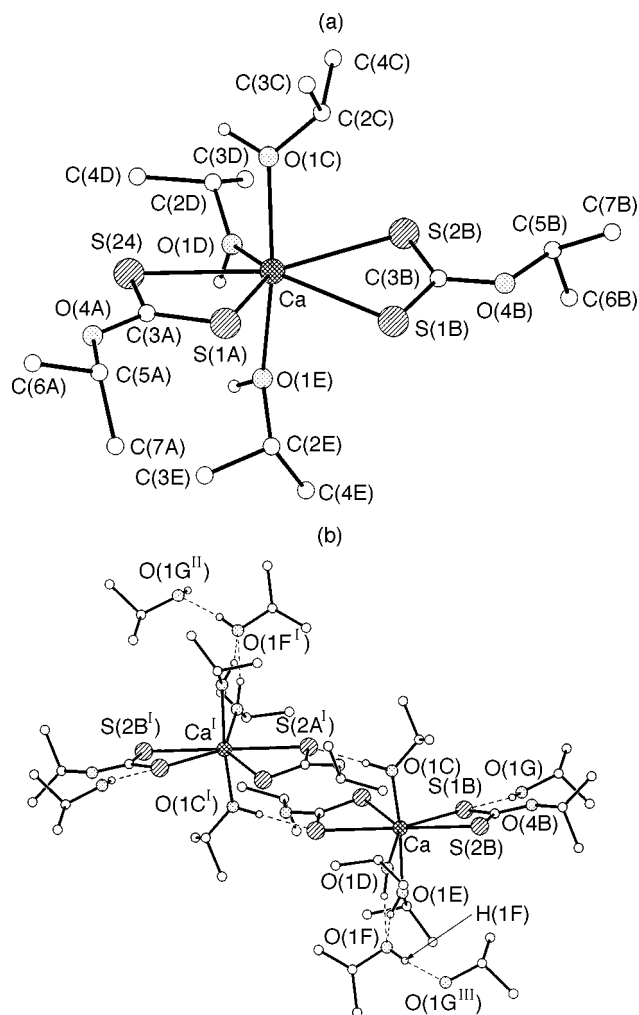
characterised dithiocarbonato complexes [Ca(S$_2$COPr^i)$_2$(Pr^{i}OH)$_3$] **6** and [{Ba(S$_2$COEt)$_2$}$_\infty$] **4**. The increasing size of the metal ion [from Ca (1.06) to Ba (1.43) Å] results in polymerisation. The seven-co-ordinate calcium ion in **6** is able to achieve co-ordinative saturation by co-ordination through the two sulfur atoms of the two dithiocarbonato ligands and three Pr^{i}OH molecules. The barium ion in **4** is in a nine-co-ordinate environment with S$_2$C(OEt)$^-$ ligands bridging adjacent barium ions forming polymeric sheets. In the previously reported alkyl thiocarbonato Group 2 complexes as well as in **6** all complexes incorporated alcohol molecules in their co-ordination sphere, in order to achieve co-ordinative saturation. Interestingly, the crystal structure of **4** shows that co-ordinative saturation is achieved by utilising the bridging capability of the ethyl dithiocarbonato ligand. The OCS(OR)$^-$ ligand in the previously studied alkyl thiocarbonato complexes, demonstrated a variety of bonding motifs, monodentate, bidentate or bridging two adjacent metal ions.[14] In this research the S$_2$C(OPr^i)$^-$ ligand has proved to be flexible, adopting different co-ordination modes but also bridging three metal ions.

Acknowledgements

Table 4 Crystal data and structure refinement details for compounds **4** and **6**

	4	**6**
Formula	$C_6H_{10}BaO_2S_4$	$C_{23}H_{54}CaO_7S_4$
M_r	379.72	610.98
Crystal system	Monoclinic	Triclinic
Space group	$P2_1/c$ (no. 14)	$P\bar{1}$ (no. 2)
$a/\text{Å}$	10.2864(11)	9.611(2)
$b/\text{Å}$	11.3404(14)	12.741(3)
$c/\text{Å}$	10.8724(14)	16.012(3)
$\alpha/°$		92.33(2)
$\beta/°$	108.885(8)	103.74(2)
$\gamma/°$		112.00(2)
$U/\text{Å}^3$	1200.0(2)	1747.5(6)
Z	4	2
$D_c/\text{Mg m}^{-3}$	2.102	1.161
$F(000)$	728	664
Crystal size/mm	$0.28 \times 0.28 \times 0.12$	$0.56 \times 0.50 \times 0.48$
$\lambda/\text{Å}$	0.710 73	0.710 73
$\mu(\text{Mo-K}\alpha)/\text{mm}^{-1}$	3.973	0.451
θ Range/°	2.09 to 24.99	1.32 to 25.00
hkl Ranges	-1 to 12, -13 to 1, -12 to 12	-1 to 11, -14 to 14, -19 to 18
Reflections collected	2766	7325
Unique reflections	2115	6123
Minimum and maximum transmission	0.724/0.811	0.500/0.861
Data, restraints, parameters	2115, 0, 118	6119, 0, 330
Goodness of fit on F^2, S	1.058	1.026
Final $R1$, $wR2$		
$\quad I > 2\sigma(I)$	0.0217, 0.0512	0.0402, 0.0731
$\quad$ All data	0.0257, 0.0534	0.0703, 0.0925
Weighting, w^{-1}	$\sigma^2(F_o)^2 + (0.0311P)^2 + 0.3023P$	$\sigma^2(F_o)^2 + (0.0283P)^2 + 0.6910P$
Largest peak and hole/e Å^{-3}	0.500, -0.535	0.248, -0.226

$S = [\Sigma w(F_o^2 - F_c^2)^2/(n - p)]^{\frac{1}{2}}$, $R1 = \Sigma||F_o| - |F_c||/\Sigma|F_o|$, $wR2 = \Sigma w(F_o^2 - F_c^2)^2/\Sigma[w(F_o^2)^2]^{\frac{1}{2}}$, $P = [\max(F_o^2, 0) + 2(F_c^2)]/3$ where n = number of reflections and p = total number of parameters.

References

1 J. A. Ibers, *Chem. Soc. Rev.*, 1982, **11**, 57.
2 K. K. Pandey, *Coord. Chem. Rev.*, 1995, **140**, 37.
3 I. S. Butler and A. E. Fenster, *J. Organomet. Chem.*, 1974, **66**, 161.
4 I. S. Butler, *Acc. Chem. Res.*, 1977, **10**, 359.
5 P. V. Ianeff, *Coord. Chem. Rev.*, 1977, **23**, 183.
6 H. Werner, *Coord. Chem. Rev.*, 1982, **43**, 165.
7 M. F. Lappert, *Adv. Organomet. Chem.*, 1967, **5**, 257.
8 SHELXTL, PC version 5.03, Siemens Analytical Instruments Inc., Madison, WI, 1994.
9 S. A. S. Miller, Ph. D. Thesis, Imperial College, London, 1995; D. J. Otway, Ph. D. Thesis, Imperial College, London, 1994.
10 A. J. Goodsel and G. Blyholder, *J. Am. Chem. Soc.*, 1972, **94**, 6725; L. J. Bellamy, *The infrared spectra of complex molecules*, 2nd edn., Wiley, New York, 1958, pp. 353–356; C. N. R. Rao and R. Venkatarachavan, *Spectrochim. Acta*, 1962, **18**, 541; G. W. Watt and B. J. McCormick, *Spectrochim. Acta*, 1965, **21**, 753; L. H. Little, G. W. Poling and J. Leja, *Can. J. Chem.*, 1961, **39**, 745; N. B. Colthur and L. Porter-Powell, *Spectrochim. Acta, Part A*, 1987, **43**, 317.
11 V. C. Arunasalam, Ph. D. Thesis, Imperial College, London, 1995.
12 N. N. Greenwood and A. Earnshaw, *Chemistry of the Elements*, Pergamon, Oxford, 1984, pp. 803–806.
13 V. C. Arunasalam, D. M. P. Mingos, J. C. Plakatouras, I. Baxter, M. B. Hursthouse and K. M. A. Malik, *Polyhedron*, 1995, **14**, 1105.
14 I. K. Bezougli, A. Bashall, M. McPartlin and D. M. P. Mingos, *J. Chem. Soc., Dalton Trans.*, 1997, **2**, 287; preceding paper.